Application of Trajectory Surface Hopping to the Study of Intramolecular Electron Transfer in Polyatomic Organic Systems

Garth A. Jones, Barry K. Carpenter,*,[1] and Michael N. Paddon-Row*

Contribution from the School of Chemistry, University of New South Wales, Sydney 2052, Australia

Received October 30, 1997. Revised Manuscript Received April 2, 1998

Abstract: An implementation of the trajectory surface hopping model is described that can be used to investigate hole or electron transfer in medium-sized organic molecules (up to about 50 atoms). The procedure employs direct dynamics with semiempirical (AM1) estimation of potential energy and its derivatives. The calculations involve configuration interaction between the lowest energy configurations and use the Landau−Zener model to estimate probabilities of hole or electron transfer at each site of avoided crossing between the diabatic configurations. In the present paper, the principles of the model are described and some qualitative insights based on single trajectories are discussed. A method for implementing a somewhat more rigorous version, using ensembles of trajectories, is also described. Application of the model to hole transfer in bridged policyclic radical cations reveals that the common assumption of a single, well-defined frequency for the encounter with the avoided-crossing region is sometimes justified but sometimes not. Support is also found for the concept of interference between hole-transfer paths within policyclic molecules—an idea that had been based on Koopmans' theorem analyses in earlier work.

We describe here the implementation of a trajectory surface hopping[2] (TSH) model that promises to afford new insight into intramolecular electron transfer (ET) in medium-sized organic molecules (up to about 50 atoms). The procedure involves running direct, classical molecular dynamics (MD) calculations on the molecule or ion of interest. The MD calculations use semiempirical molecular orbital theory, including configuration interaction (CI) between the lowest energy electronic configurations. The use of the direct-dynamics procedure, including CI, permits extension of the TSH approach to complex polyatomic systems without need to specify the hypersurface of avoided crossing of diabatic states.[2] Although more rigorous models have been developed for treating the dynamics of small systems on multiple electronic surfaces,[3] the present more approximate method has the virtue of ready applicability to the relatively large molecules of interest to the organic and biological chemistry community, while still providing qualitatively meaningful conclusions. Our optimism is reinforced by the recent successful application of TSH methods, using a hybrid ab initio quantum-mechanical/force-field potential, to study the dynamics of photochemical reactions of medium-sized organic molecules.[4] Indeed, full ab initio semiclassical TSH-based dynamics calculations have also been carried out on the photoisomerization of a simple retinal chromophore model, albeit within a highly restricted region of phase space.[5]

We believe there is a need for approximate methods of the kind presented here because, as we hope to show, there can be dynamically important issues that arise for ET in larger molecules. These phenomena would not be identified by the common, nondynamic models for ET[6] and may not be computationally tractable if treated by the more rigorous dynamic methods. For the radical ions **1**−**4**, the present method takes several hours of CPU time per trajectory on a fast workstation such as the SGI r10000. If the dynamics of such systems are to be investigated with a statistically significant sample of initial conditions, the more extensive calculation required for the higher-level models[3] may put them outside of the realm of computational convenience, although we are currently investigating that question.

(1) Permanent address: Department of Chemistry, Baker Laboratory, Cornell University, Ithaca, NY 14853-1301.

(2) (a) Tully, J. C.; Preston, R. K. *J. Chem. Phys.* **1971**, *55*, 562. (b) Miller, W. H.; George, T. F. *J. Chem. Phys.* **1972**, *56*, 5637. (c) Tully, J. C. *Ber. Bunsen-Ges. Phys. Chem.* **1973**, *77*, 557. (d) Stine, J. R.; Muckerman, J. T. *J. Chem. Phys.* **1976**, *65*, 3975. (e) Tully, J. C. In *Dynamics of Molecular Collisions, Part B*; Miller, W. H., ed.; Plenum: New York, 1976; p 217. (f) Kuntz, P. J.; Kendrick, J.; Whitton, W. N. *Chem. Phys.* **1979**, *38*, 147. (g) Blais, N. C.; Truhlar, D. G. *J. Chem. Phys.* **1983**, *79*, 1334. (h) Parlant, G.; Gisalson, E. A. *J. Chem. Phys.* **1989**, *91*, 4416. (j) Mead, C. A.; Truhlar, D. G. *J. Chem. Phys.* **1986**, *84*, 1055. (k) Stine, J. R.; Muckerman, J. T. *J. Chem. Phys.* **1986**, *84*, 1056. (l) Chapman, S. *Adv. Chem. Phys.* **1992**, *82*, 423.

(3) (a) Tully, J. C. *J. Chem. Phys.* **1990**, *93*, 1061. (b) Webster, F. A.; Rossky, P. J.; Friesner, R. A. *Comput. Phys. Commun.* **1991**, *63*, 494. (c) Coker, D. F. In *Computer Simulation in Chemical Physics*; Allen, M. P., Tildesley, D. J., Eds.; Kluwer Academic Publishers: Dordrecht, The Netherlands; 1993; Vol. 397. (d) Hammes-Schiffer, S.; Tully, J. C. *J. Chem. Phys.* **1994**, *101*, 4657. (e) Hammes-Schiffer, S.; Tully, J. C. *J. Phys. Chem.* **1995**, *99*, 5793. (f) Martinez, T. J.; Levine, R. D. *J. Chem. Soc., Faraday Trans.* **1997**, *93*, 941. (g) Prezhdo, O. V.; Rossky, P. J. *J. Chem. Phys.* **1997**, *107*, 825.

(4) (a) Smith, B. R.; Bearpark, M. J.; Robb, M. A.; Bernardi, F.; Olivucci, M. *Chem. Phys. Lett.* **1995**, *242*, 27. (b) Bearpark, M. J.; Bernardi, F.; Olivucci, M.; Robb, M. A.; Smith, B. R. *J. Am. Chem. Soc.* **1996**, *118*, 5254. (c) Clifford, S.; Bearpark, M. J.; Bernardi, F.; Olivucci, M.; Robb, M. A.; Smith, B. R. *J. Am. Chem. Soc.* **1996**, *118*, 7353. (d) Bearpark, M. J.; Bernardi, F.; Clifford, S.; Olivucci, M.; Robb, M. A.; Smith, B. R.; Vreven, T. *J. Am. Chem. Soc.* **1996**, *118*, 169.

(5) Vreven, T.; Bernardi, F.; Garavelli, M.; Olivucci, M.; Robb, M. A.; Schlegel, H. B. *J. Am. Chem. Soc.* **1997**, *119*, 12687.

(6) (a) Marcus, R. A. *J. Chem. Phys.* **1956**, *24*, 966. (b) Marcus, R. A. *J. Chem. Phys.* **1956**, *24*, 979. (c) McConnell, H. M. *J. Chem. Phys.*. **1961**, *35*, 508. (d) Marcus, R. A.; Sutin, N. *Biochim. Biophys. Acta* **1985**, *811*, 265. (e) Hush, N. S. *Coord. Chem. Rev.* **1985**, *64*, 135. (f) Naleway, C. A.; Curtiss, L. A.; Miller, J. R. *J. Phys. Chem.* **1991**, *95*, 8434. (g) Jordan, K. D.; Paddon-Row: M. N. *Chem. Rev.* **1992**, *92*, 395. (h) Liang, C.; Newton, M. D. *J. Phys. Chem.* **1992**, *96*, 2855. (i) Paddon-Row: M. N. *Acc. Chem. Res.* **1994**, *27*, 18. (j) Cave, R. J.; Newton, M. D. *Chem. Phys. Lett.* **1996**, *249*, 15.

S0002-7863(97)03753-0 CCC: $15.00
Published on Web 05/13/1998

In the model used here, odd-electron species are treated by the "half-electron" approximation,[7] since this has previously been shown[8] to provide an operationally useful way to avoid the problem of doublet instability that is commonly encountered with ROHF or UHF wave functions for radicals and radical ions.

Introduction and Definition of Terms

In the present work, we seek to simulate the degenerate hole transfer (HT) in radical ions **1**−**4**. These structures have been

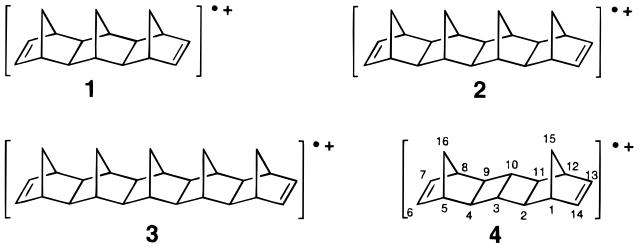

subjected to theoretical scrutiny by other techniques[9] and represent prototypes of systems for which experimental studies of electron-transfer rates have been carried out.[6i,10]

It is common to think of the hole-transfer reaction in such species as occurring at an avoided crossing between diabatic (localized) electronic states. The concept can be depicted schematically as shown in Figure 1. According to both the AM1-CI model and UHF ab initio methods, the radical ions **1**−**4** all have charge-localized, C_s-symmetry structures as their global potential-energy minima (see Supporting Information for details). In these geometries, the overall electronic wave function for the system would be reasonably well approximated by a diabatic function that located the hole in one of the two π bonds. However, as the system progresses along the reaction coordinate for hole transfer—a geometrical distortion that reduces the length of the one-electron π bond while increasing the length of the two-electron π bond—the energies of the diabatic wave functions corresponding to localization of the hole in the left or the right π bond (ψ_L and ψ_R, respectively) approach each other in energy. As they do so, the single-configuration, diabatic wave functions become less and less satisfactory descriptions of the system. Finally, in the center of the diagram, the overall wave function must consist of equal-magnitude contributions from the diabatic configurations in order to conform to the symmetry (ideally C_{2v} for radical ions **1**−**4**) of the nuclear positions. Thus, at the point where the energies of the diabatic wave functions would have crossed, two new adiabatic states with wave functions $(\psi_L + \psi_R)/\sqrt{2}$ and $(\psi_L - \psi_R)/\sqrt{2}$ (assuming orthogonal diabatic functions) appear, and the crossing is avoided because these adiabatic states have different energies. At the avoided crossing, the positive charge associated with the hole is equally distributed between left and right sides of the radical ion in both adiabatic states. The CI matrix element that couples the diabatic states, H_{12}, is equal to half the energy gap between adiabatic states at the avoided crossing.

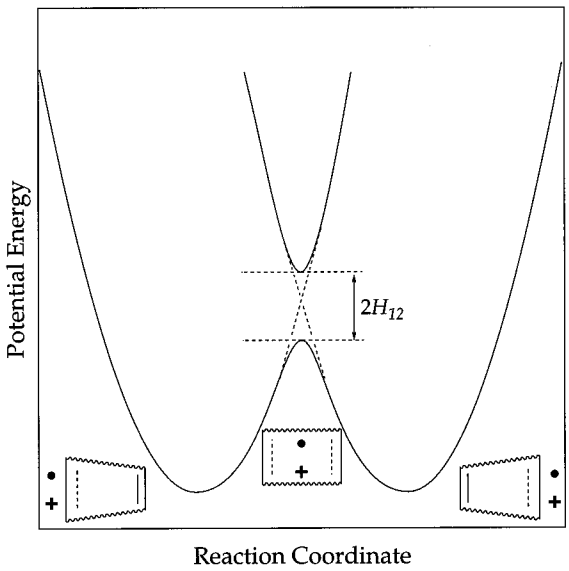

Figure 1. Schematic representation of the adiabatic potential energy surfaces for hole transfer in radical ions **1**−**4**. The adiabatic electronic states can be thought of as arising from a mixing of diabatic wave functions corresponding to localization of the hole in the left and the right π bond. H_{12} is matrix element that describes the coupling between these diabats.

There exists a technical detail in the actual calculations used here that represents a potential source of confusion to this relatively straightforward picture. With the commonly used MO methods, including the AM1 model employed for the present work, the single-configuration wave functions are themselves delocalized. The two adiabatic states (solid curves) in Figure 1 would be fairly well approximated by such single-configuration delocalized MOs. However, if CI is carried out between the delocalized MOs, the resulting states will be identical to those derived from the CI between diabatic configurations. This fact allows us to retain the description of a crossing between diabatic states in the following text, even though no diabatic wave functions were ever used. When we speak of adiabatic states, the implication will be that we mean those states generated by CI.

The behavior of the system during the MD simulations can conveniently be discussed with a diagram (Figure 2) derived from the avoided-crossing model. The three horizontal lines in Figure 2 represent the total (potential plus kinetic) energies of different hypothetical trajectories. In trajectory A, the total energy is insufficient to surmount the barrier to HT on the lower adiabatic PES. No HT can occur for this trajectory (except by quantum-mechanical tunneling which is not included in our classical-dynamics simulation). The curved arrow surrounding the energy level A depicts the dynamic behavior of the system. The trajectory consists of a simple vibration where direction of motion along the reaction coordinate reverses each time a potential-energy barrier is encountered.

Trajectory B has sufficient total energy to surmount the barrier, and so it will lead directly to HT. It does not, however, have enough energy to gain access to the upper adiabatic PES.

(7) (a) Nesbet, R. K. *Proc. R. Soc.* **1955**, *A230*, 312. (b) Dewar, M. J. S.; Hashmall, J. A.; Venier, C. G. *J. Am. Chem. Soc.* **1968**, *90*, 1953.

(8) (a) Rauhut, G.; Clark, T. *J. Am. Chem. Soc.* **1993**, *115*, 9127. (b) Rauhut, G.; Clark, T. *J. Chem. Soc., Faraday Trans.* **1994**, *90*, 1783.

(9) (a) Paddon-Row: M. N. *Acc. Chem. Res.* **1982**, *15*, 245. (b) Paddon-Row: M. N.; Wong, S. S. *Chem. Phys. Lett.* **1990**, *167*, 432. (c) Jordan, K. D.; Paddon-Row: M. N. *J. Phys. Chem.* **1992**, *96*, 1188. (d) Shephard, M. J.; Paddon-Row: M. N.; Jordan, K. D. *J. Am. Chem. Soc.* **1994**, *116*, 5328. (e) Shephard, M. J.; Paddon-Row: M. N. *J. Phys. Chem.* **1995**, *99*, 17497. (f) Paddon-Row: M. N.; Shephard, M. J. *J. Am. Chem. Soc.* **1997**, *119*, 5355.

(10) (a) Oevering, H.; Paddon-Row: M. N.; Heppener, M.; Oliver, A. M.; Cotsaris, E.; Verhoeven, J. W.; Hush, N. S. *J. Am. Chem. Soc.* **1987**, *109*, 3258. (b) Penfield, K. W.; Miller, J. R.; Paddon-Row: M. N.; Cotsaris, E.; Oliver, A. M.; Hush, N. S. *J. Am. Chem. Soc.* **1987**, *109*, 5061. (c) Oliver, A. M.; Craig, D. C.; Paddon-Row: M. N.; Kroon, J.; Verhoeven, J. W. *Chem. Phys. Lett.* **1988**, *150*, 366. (d) Kroon, J.; Verhoeven, J. W.; Paddon-Row: M. N.; Oliver, A. M. *Angew. Chem., Int. Ed. Engl.* **1991**, *30*, 1358.

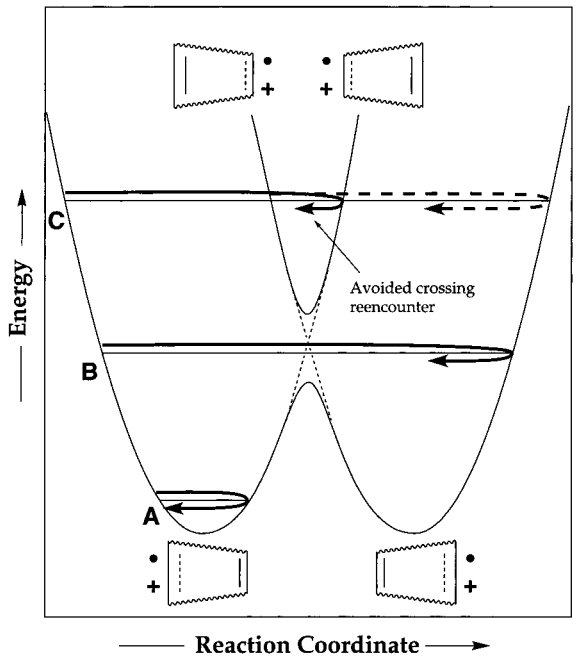

Figure 2. Behavior of various trajectories (curved arrows) on the adiabatic surfaces shown in Figure 1. For trajectory A, the total energy (potential energy plus kinetic energy in the reaction coordinate) is insufficient to surmount the barrier on the lower surface and so hole transfer cannot occur without tunneling, which is neglected in our model. For trajectory B, the total energy is sufficient to cross the barrier on the lower surface but insufficient to provide access to the upper surface. For trajectory C, the total energy is sufficient to allow access to the upper surface and so two outcomes are possible. If a transition to the upper electronic state occurs, hole transfer is inhibited, but the system soon encounters a PE barrier which causes it to return rapidly to the region of the avoided crossing. This is shown by the solid curved arrow. If the system stays in the lower electronic state, hole transfer analogous to that for trajectory B will occur. This is depicted by the dashed curved arrow.

Like B, trajectory C has sufficient energy to cause HT, but it is now energetic enough to undergo TSH and switch adiabatic electronic states. Thus, trajectory C bifurcates in the region of the avoided crossing. Along one of the resulting trajectory branches, denoted by a dashed line, TSH does not occur and it resembles qualitatively the trajectory B; that is, HT will occur.

However, the other trajectory branch, denoted by the extended solid arrow, results from the system undergoing TSH and it evolves along the upper, single-well potential energy surface. In this state, the trajectory now oscillates about the C_{2v} energy minimum of this surface, which lies in the region of the avoided crossing. The trajectory therefore makes repeated encounters with the avoided crossing, two for each completed oscillation.

On each encounter with the avoided crossing, the system has a probability of escaping from the confines of the upper surface by undergoing TSH to the lower, double-well surface. Two possible trajectories emerge from such an occurrence, one leading to reactant and the other to product. Which one of these trajectories the system will actually follow is determined by the direction that the trajectory is taking on the upper surface, just prior to the TSH.

If the upper surface trajectory encounters the avoided crossing while it is proceeding along the reaction coordinate of Figure 2 from left to right, then, following TSH, it will carry the system in the direction of product and HT will occur, since this is in the direction of the momentum of the system projected along the reaction coordinate. If, on the other hand, the upper surface trajectory is moving from right to left then, following TSH, it will proceed to reactant and HT does not yet take place. This trajectory will then "bounce" off the left-hand wall of the of the reactant well and eventually return to the avoided crossing region, where again, it has the choice of undergoing HT or TSH. In the more rigorous version (vide infra) of our implementation of the MD method, such a trajectory (and all other types of trajectories for that matter) is followed until HT takes place, at which point it is terminated.

In summary, any trajectory which ends up on the upper surface by TSH makes repeated encounters with the avoided crossing region and this pattern is terminated only by the occurrence of TSH to the lower surface.

For trajectories such as C, in our treatment, the probability of HT at a locus of avoided crossing between diabatic states is assessed by use of the Landau−Zener model.[11] The details of the calculation of Landau−Zener probabilites are discussed below. Here, we simply point out the implications of the potential multiple encounters with avoided crossings that can occur for trajectories of type C that switch to the higher electronic state on the first encounter. For the sake of simplicity, we will assume that the probability, p, of the system remaining on its present adiabatic surface as it passes through an avoided crossing is the same for each encounter. The multiple encounters occurring on the upper adiabatic surface are such that the even-numbered ones (counting the initial transition from the lower surface to the upper as encounter number 1) lead to reactant formation following TSH to the lower surface (the trajectory is moving toward the left on the upper surface) and the odd numbered ones to HT (the trajectory is moving toward the right on the upper surface). Thus, only trajectories on the upper surface that have experienced an odd number of encounters can lead directly to HT formation by a TSH mechanism.

The first encounter, resulting from the initial trajectory proceeding from reactant to the avoided crossing region on the lower surface has, by definition, a probability p of effecting HT. The fraction $1 - p$ that experiences a transition to the upper surface must undergo two more encounters with the avoided-crossing region before it can lead to HT by TSH. The probability of such an event is $p(1 - p)^2$. As discussed above, HT via the upper electronic surface requires an odd number avoided-crossing encounters. The total probability, P, of conversion from reactant well to product well on the lower surface is thus described by a series of the form:

$$P = p + p(1 - p)^2 + p^3(1 - p)^2 + p^5(1 - p)^2 + ...$$

which converges to $2p/(1 + p)$ since $0 \leq p \leq 1$. This sum excludes trajectories that return at least once to reactant (via TSH from the upper surface, vide supra) before proceeding to HT.

In a proper, quantum-mechanical description of this process, the wave packets corresponding to the multiple encounters with the avoided crossing could interfere with each other and thereby influence the total probability of HT.[3] In the present model, the time-dependent vibronic wave function is never computed and so no such interference can be seen in the simulation. However, we believe that the neglect of interference is justifiable for the following reasons. First, a number of studies have shown that coupling of the reaction coordinate to a bath of oscillators, whether intra- or intermolecular, quickly causes dephasing of

(11) (a) Landau, L. D. *Phys. Z. Sowjetunion* **1932**, *2*, 46. (b) Zener, C. *Proc. R. Soc. (London)* **1932**, *A137*, 696.

the vibronic wave function.[12] For molecules of the size considered here, loss of coherence can be expected to be very fast. Second, while the one-dimensional reaction coordinate of Figure 2 would seem to imply that the second encounter of trajectory C with the avoided crossing occurs at the same geometrical coordinates as the first encounter, in a higher-dimensional representation, this is not the case. During the brief period that the trajectory is evolving on the upper surface, many other geometrical coordinates (notably C−H bond lengths) are changing, with little influence on energy the gap between electronic states. Consequently, each encounter with an avoided-crossing region occurs at a substantially different geometry, and hence, a substantially difference place on the upper potential energy hypersurface. The opportunity for wave packet interference is consequently lower than it seems to be in the one-dimensional representation. Finally, one can anticipate that averaging over a variety of initial conditions for the MD simulation would wash out any residual quantum-mechanical interference that might be seen in reactions from single initial states.

Description of the Theoretical Model

The principles of the model are perhaps best portrayed by presenting a detailed description of its application to the dynamics of intramolecular HT in the radical ion **1**. Semiempirical calculations at the AM1[13] level with 2 × 2 CI suggest that ion **1** has a localized, C_s-symmetry structure as the global minimum but that there exists also a delocalized, C_{2v}-symmetry structure as a shallow local minimum[14] on the potential energy surface surface (PES). The difference in energy[15,16] between the two structures is found to be 1.38 kcal/mol. Ab initio MO calculations[17a] at the UHF/6-31G(d) level, as well as UB3LYP/6-31G(d) hybrid HF/density-functional calculations[17b,c] concur with the AM1 model that the C_{2v} structure is a minimum on the PES. However, the UHF calculations place it anomalously high above the C_s structure, whereas the UB3LYP model makes it the global minimum. Neither of these ab initio results seems intuitively reasonable. Details of both ab initio and semiempirical calculations can be found in the Supporting Information.

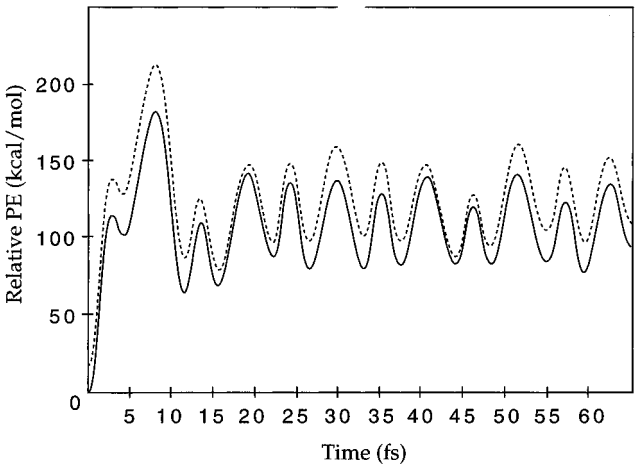

Figure 3. Time dependence of the energies of the two lowest electronic states of radical ion **1**, from a trajectory with zero-point energy in all normal modes. Energies are relative to that for the lower electronic state of the C_s stationary point.

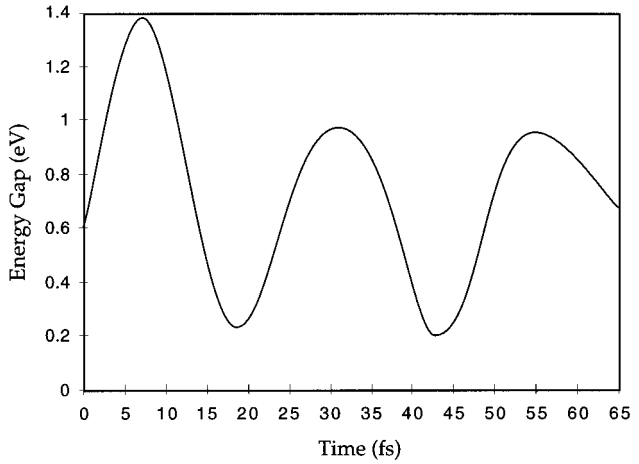

Figure 4. Time dependence of the difference in energy between the two lowest electronic states of radical ion **1**, from a trajectory with zero-point energy in all normal modes.

The dynamic reaction coordinate[18] routine that is part of the MOPAC93 program was used to run a classical trajectory calculation starting from the C_s stationary point for **1** with zero-point vibrational energy supplied to each of the normal modes of the ion. The energies[15] of the two electronic states relevant for the hole-transfer process (in this case, and usually, those being the two lowest states) could be followed as a function of time, with the result shown in Figure 3. This is a typical outcome of an MD calculation on a polyatomic molecule—the only special feature being that the energies of two electronic states are tracked instead of one. It may not be obvious that there is useful information contained in Figure 3, but the potential utility of the calculation is revealed if one recasts the results as a plot of the absolute value of the difference in energy between the two states as a function of time (Figure 4). This graph reveals that the energy gap, $\Delta E(t)$, between the electronic states is modulated at much lower frequency than the total energies of the states are.

An obvious interpretation of this result is that not all vibrational normal modes influence the difference in energy between the electronic states equally. In fact, the first 18 fs of the $\Delta E(t)$ function in Figure 4 can be fit extremely well by a

(12) (a) Schneider, R.; Domcke, W.; Köppel, H. *J. Chem. Phys.* **1990**, *92*, 1045. (b) Bixon, M.; Jortner, J. *J. Chem. Phys.* **1997**, *107*, 1470.

(13) Dewar, M. J. S.; Zoebisch, E. G.; Healy, E. F.; Stewart, J. J. P. *J. Am. Chem. Soc.* **1985**, *107*, 3902. Calculations were carried out with Revision 2 of the MOPAC93 package (J. J. P. Stewart, Fujitsu Limited, Tokyo, Japan, 1993).

(14) The exact depth of the local minimum in the AM1 model is not known. Repeated attempts to locate the transition structure between C_s and C_{2v} minima were unsuccessful, presumably because the gradients were too small to be outside of the error in their estimation.

(15) Because the AM1 method is parametrized against experimental heats of formation, it actually computes enthalpies rather than potential energies. In this paper, we equate relative enthalpies of isomeric species with their relative potential energies. This leads to an unavoidable ambiguity in the discussion of zero-point energies, but the errors associated with the approximation are, we judge, unlikely to be the most severe in the present model.

(16) Because the molecular dynamics routine does not make use of analytical CI gradients, all geometry optimizations and frequency calculations were carried out without them (MOPAC keyword NOANCI). In this way one ensures that the stationary points and normal modes used to generate the initial conditions are the most appropriate for the trajectory calculations that follow.

(17) (a) Gaussian 94, Revision D.3: Frisch, M. J.; Trucks, G. W.; Schlegel, H. B.; Gill, P. M. W.; Johnson, B. G.; Robb, M. A.; Cheeseman, J. R.; Keith, T.; Petersson, G. A.; Montgomery, J. A.; Raghavachari, K.; Al-Laham, M. A.; Zakrzewski, V. G.; Ortiz, J. V.; Foresman, J. B.; Cioslowski, J.; Stefanov, B. B.; Nanayakkara, A.; Challacombe, M.; Peng, C. Y.; Ayala, P. Y.; Chen, W.; Wong, M. W.; Andres, J. L.; Replogle, E. S.; Gomperts, R.; Martin, R. L.; Fox, D. J.; Binkley, J. S.; Defrees, D. J.; Baker, J.; Stewart, J. P.; Head-Gordon, M.; Gonzalez, C.; Pople, J. A. Gaussian, Inc., Pittsburgh, PA, 1995. (b) Becke, A. D. *J. Chem. Phys.* **1993**, *98*, 5648. (c) Lee, C.; Yang, W.; Parr, R. G. *Phys. Rev.* **1988**, *37*, 785.

(18) Stewart, J. J. P.; Davis, L. P.; Burggraf, L. W. *J. Comput. Chem.* **1987**, *8*, 1117.

simple sine function of frequency 1458 cm^{-1}. (The reason for not trying to fit beyond 18 fs will be discussed below.) Early in this trajectory, it thus appears as if a single mode of frequency 1458 cm^{-1} is the only one to have any significant modulating effect on ΔE. A candidate for this mode is clear. At the geometry of the C_s global minimum, the two states are each dominated by a single diabatic configuration. The lower energy state is dominated by a configuration in which the hole is localized on the longer of the two carbon−carbon π bonds. In the higher energy state the dominant configuration localizes the hole in the shorter π bond. The antisymmetric combination of π-bond stretching motions, which tends to equalize the lengths of these bonds in one phase of its excursion, can be expected to reduce the energy gap between the states and is therefore a good candidate for the mode revealed in Figure 4. The harmonic vibration frequency[14] for this mode is found to be 1476 cm^{-1} in the AM1-CI calculations. The 18-cm^{-1} discrepancy between this value and the one derived from Figure 4 can presumably be attributed to the anharmonicity that results from the strong coupling of this mode to the reaction coordinate for HT, vide infra.

Beyond about 19 fs, the curve in Figure 4 looks much less sinusoidal than the early portion does. That is because at 18.5 fs HT is found to occur (as judged by the change in charges on the atoms; see Figure 1).

For the trajectory under discussion, the AM1 calculations apparently place the barrier to HT below the ZPE of the mode that makes the principal contribution to the reaction coordinate. In other words, the present trajectory corresponds to B or C in Figure 2. The loss of periodic motion that accompanies HT is to be expected because the sudden change in force constants that results from the charge migration tends to dephase the coupled oscillators.

Even if the AM1 MD calculations were exactly accurate in their description of the time dependence of the lowest two electronic states of **1**, one could only conclude that HT would in fact occur after 18.5 fs for this trajectory if the situation were that depicted by B in Figure 2. If the total energy were sufficient to provide access to the upper adiabatic electronic state, as shown in C of Figure 2, the probability of HT would not be unity. In our treatment, the magnitude of this probability is assessed by use of the Landau−Zener model,[9] as detailed below. The behavior of the system if HT did not occur is determined by running the dynamics calculation after the 18.5-fs point using the higher energy root of the 2×2 CI determinant to determine the forces.[19] This TSH to the adiabatic state of higher potential energy must be accompanied by a discontinuous change in the momenta of the atoms in order to ensure total energy conservation. A number of procedures have been suggested for accomplishing this momentum correction.[3] In the present work, we have used the Miller and George model, which is given by eq 1.[2b]

$$\mathbf{p}^{(2)} = \mathbf{p}^{(1)} \pm \mathbf{n}\frac{\mathbf{n}\mathbf{M}^{-1}\mathbf{p}^{(1)}}{\mathbf{n}\mathbf{M}^{-1}\mathbf{n}}\left[1 - \left(1 - 2\Delta E\frac{\mathbf{n}\mathbf{M}^{-1}\mathbf{n}}{(\mathbf{n}\mathbf{M}^{-1}\mathbf{p}^{(1)})^2}\right)^{1/2}\right] \quad (1)$$

The vectors $\mathbf{p}^{(1)}$ and $\mathbf{p}^{(2)}$ specify the momenta of the atoms respectively before and after the switch between adiabatic surfaces. Matrix $\mathbf{M}$ is the diagonal mass matrix, and ΔE is the potential energy difference (positive for a transition from the lower to the higher energy state, negative for the reverse) between the surfaces at the time of the transition. The parameter $\mathbf{n}$ is a unit vector specifying the direction of the instantaneous reaction coordinate for hole or ET. If the transition between adiabatic surfaces occurred exactly at a first-order stationary point on the lower surface, $\mathbf{n}$ would be along the direction of the normal mode of imaginary frequency. However, in general, the transition will not occur at a stationary point, and so specification of $\mathbf{n}$ by normal-mode analysis is not straightforward. Fortunately, Miller and George have shown that $\mathbf{n}$ can be found by tracking any property of the system that is symmetrically positive on one side of the transition, zero at the point of transition, and negative on the other side.[2b] We have used the charges on the carbons of the π bonds in radical ion to provide us with this information. Thus we numerically evaluate the vector $\nabla(\Delta q(\xi))$, where ξ are the Cartesian coordinates of the atoms, and for radical ion **1**

$$\Delta q(\xi) = q_{13} + q_{14} - q_6 - q_7 \quad (2)$$

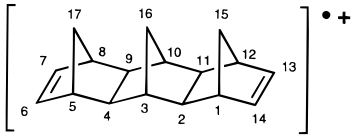

The q_i are the calculated charges on carbons i in the ground-state structure corresponding to the avoided crossing. The unit vector $\mathbf{n}$ is then taken to be along the direction of $\nabla(\Delta q(\xi))$. The ambiguity in the sign of the momentum correction in eq 1 arises, in the general case, because of the arbitrary location of the hole prior to the transition, and hence the arbitrary sign of Δq. The ambiguity is resolved by choosing the sign in eq 1 that leads to conservation of total energy after the transition.

That $\mathbf{n}$ is quite well located by this procedure is shown by carrying out the calculation of $\nabla(\Delta q(\xi))$ on the C_{2v} local-minimum structure for radical ion **1** and then computing angles of this vector with the momentum vectors corresponding to the normal modes. The results are shown in Table 1 in the Supporting Information. The vector $\nabla(\Delta q(\xi))$ is found to be nearly orthogonal to all normal modes except one, that being the b_2-symmetry combination of π-bond stretches. The alignment with this mode and the orthogonality to the other modes are not perfect because, as described above, the C_{2v} stationary point is a shallow local minimum, not a transition structure, and so the reaction coordinate for charge transfer will be very similar to, but not identical with, the b_2 normal mode for π-bond stretching.

In the general case, the direction of vector $\nabla(\Delta q(\xi))$ need not be exactly along the instantaneous reaction coordinate because the charge differences for small displacements on either side of the critical structure need not conform to the relationship $\Delta q(\xi + \delta\xi) = -\Delta q(\xi - \delta\xi)$, but such behavior for the function used to locate $\mathbf{n}$ was assumed in the derivation of eq 1. Nevertheless, we judge that any errors in the momentum correction arising from the use of $\nabla(\Delta q(\xi))$ are likely to be small, especially because the probability of a hop to the higher energy adiabatic surface is only significant when the gap ΔE is small (vide infra), and hence when the necessary corrections to the momenta are also small.

For the particular case of the trajectory shown in Figure 4, evaluation of eq 1 leads to imaginary corrections to the momenta. This is because the trajectory has insufficient kinetic energy along the direction of the reaction coordinate to access the higher energy adiabatic surface. Thus, this trajectory

(19) In the general case, more than two configurations might need to be included in the CI, in which case the root used would be the lowest energy one of correct spin symmetry that kept the hole or electron localized at the original site.

corresponds to case B of Figure 2, and so one can now conclude that HT should indeed be judged to take place at the 18.5 fs mark.

On reflection, one can see that all trajectories having only ZPE in the normal modes of the starting structure are likely to be of type B. The antisymmetric combination of π-bond stretches, which effectively becomes the reaction coordinate, has a ZPE of 2.1 kcal/mol. This is sufficient to surmount the barrier on the lower surface (1.4 kcal/mol) but not sufficient to gain access to the higher surface which, at the C_{2v} geometry, is found to be 4.1 kcal/mol above the barrier on the lower surface. While different trajectories will encounter the avoided crossing in places where the gap is not necessarily the same as that at the C_{2v} stationary point, none is likely to have a gap as small as 0.7 kcal/mol (the maximum value allowing access to the upper surface) because the efficient through-bond coupling and relative rigidity of **1** ensure quite a large separation between the states at all energetically reasonable geometries.

Although, for radical ion **1**, it appears that few trajectories will have sufficient kinetic energy in the direction of the reaction coordinate to make the transition to the higher surface, that need not be the outcome for all molecular systems undergoing hole or ET. When access to the higher surface is energetically feasible, one needs to calculate the probability of its occurrence. This is achieved in the present work by using the Landau−Zener model (eq 3):[9]

$$P = 1 - e^{-2\pi\gamma} \qquad \gamma = \frac{{H_{12}}^2}{\hbar v|s_1 - s_2|} \tag{3}$$

P is the probability of staying on the lower adiabatic PES (corresponding to successful HT for the present problem), H_{12} is the matrix element that couples the diabatic surfaces at the avoided crossing, v is the velocity of motion along the reaction coordinate, and s_1 and s_2 are the first derivatives of the potential energies of the two diabatic states with respect to the reaction coordinate at the point of the avoided crossing.

In polyatomic systems, the utility of this formula is limited by the difficulty of assigning values to the parameters v, s_1, and s_2. However, in a dynamics calculation, one can transform these parameters into more conveniently accessible quantities. Thus, if one defines θ to be the reaction coordinate for the system, then the Landau−Zener parameters v and $|s_1 - s_2|$ can be written as

$$v = \mathrm{d}\theta/\mathrm{d}t \tag{4}$$

$$|s_1 - s_2| = \left|\frac{\mathrm{d}E_1}{\mathrm{d}\theta} - \frac{\mathrm{d}E_2}{\mathrm{d}\theta}\right| = \frac{\mathrm{d}|\Delta E_{\mathrm{diabatic}}|}{\mathrm{d}\theta} \tag{5}$$

where E_1 and E_2 are the potential energies of the two diabatic states. From this it follows that

$$v|s_1 - s_1| = \frac{\mathrm{d}\theta}{\mathrm{d}t}\frac{\mathrm{d}|\Delta E_{\mathrm{diabatic}}|}{\mathrm{d}\theta} = \frac{\mathrm{d}|\Delta E_{\mathrm{diabatic}}|}{\mathrm{d}t} \tag{6}$$

In other words, the denominator of the exponent in the Landau−Zener expression (eq 3) is just $\hbar$ times the rate of change of the energy gap between the diabatic states with respect to time, in the vicinity of the avoided crossing.[3c] This latter quantity can be estimated from the molecular dynamics, as illustrated in Figure 5.

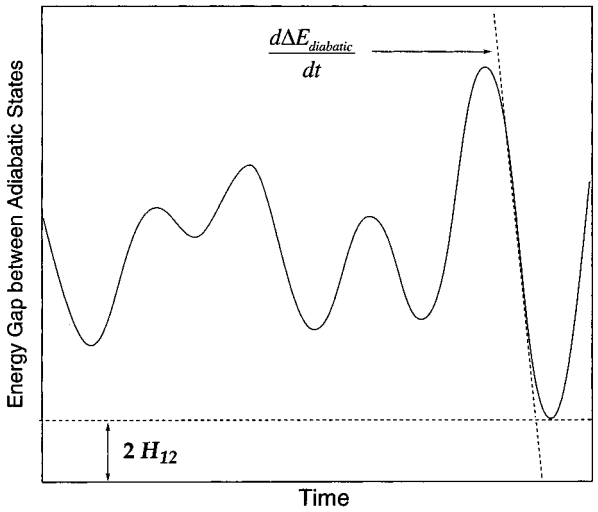

Figure 5. Schematic representation of the calculation of Landau−Zener parameters from the results of the MD simulation. See text and footnote 20 for details of the actual procedure.

The ΔE in Figure 5 is the energy gap between *adiabatic* states as a function of time. The curvature in $\Delta E_{\mathrm{adiabatic}}(t)$ that arises from configuration mixing as the avoided crossing is approached ensures that $\mathrm{d}|\Delta E_{\mathrm{adiabatic}}|/\mathrm{d}t \leqslant \mathrm{d}|\Delta E_{\mathrm{diabatic}}|/\mathrm{d}t$ at all points. Consequently, we estimate the quantity $\mathrm{d}|\Delta E_{\mathrm{diabatic}}|/\mathrm{d}t$ by finding the maximum value of $\mathrm{d}|\Delta E_{\mathrm{adiabatic}}|/\mathrm{d}t$ as the avoided crossing is approached. Since H_{12} is also available (Figure 5), being equal to $\Delta E/2$ at the time of HT,[20] one has all of the parameters necessary to compute the Landau−Zener probability.

The avoided crossing in Figure 5 is deliberately shown *not* to occur at the first minimum in $\Delta E(t)$. For radical ions such as **1**, the first encounter with an avoided crossing usually is at the first minimum in $\Delta E(t)$, but in the general case, it need not be. For conformationally flexible molecules, or molecules having symmetry prohibitions to ET in their stationary-point geometries, molecular vibrations can cause significant modulation of ΔE by changing the electronic coupling between donor and acceptor. The minima of such fluctuations could easily be confused with sites of avoided crossing were it not for the fact that the direct dynamics simulation, including CI, will invariably cause the hole or ET to take place when a genuine avoided crossing is encountered. This is, of course, signaled by an abrupt movement of charge within the system from the donor region to the acceptor region.

Adoption of Tully's "anteater" model[2a] affords the following strategy for applying these calculations to the computation of the overall rate constant for hole or ET in a molecule. One could generate a suitable set of initial conditions for the MD calculations—a sample from a quasiclassical canonical ensemble would presumably be a reasonable choice for simulation of a thermal reaction—and then use the computed Landau−Zener probability at every avoided crossing to control the dynamics. For each avoided crossing encountered in each trajectory, a randomly generated number in the interval 0−1 could be compared to the hole- or electron-transfer probability, and the result used to decide whether transfer occurred or not. If it did, the trajectory would be stopped; if not, the trajectory would be continued with a switch to the other adiabatic electronic state of the system and correction of the momenta according to eq 1

(20) In Figure 5, we show H_{12} being equal to $\Delta E/2$ at the minimum in the $\Delta E(t)$ curve. In reality, hole transfer, as monitored by atomic charges, does not have to occur exactly at the minimum, although it will always be close. We use the ΔE value at the time of hole transfer to estimate H_{12}.

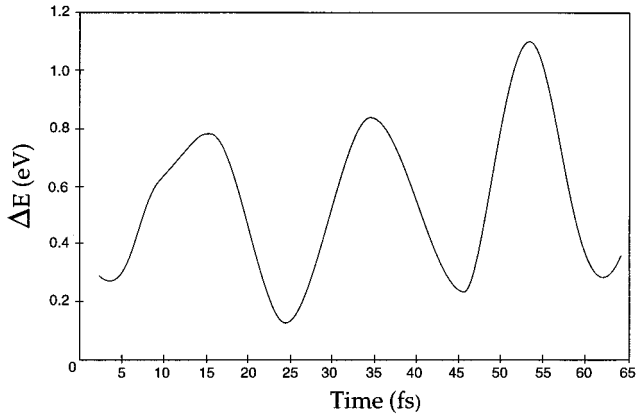

Figure 6. Time dependence of the energy gap between adiabatic states for radical ion **2** from a trajectory with just ZPE in all normal modes.

would be made. A negative value for the quantity inside the square root of eq 1 would serve to signal HT and hence cause cessation of the trajectory, since it would imply that the trajectory had too small a component of kinetic energy along the direction of the vector **n** to access the upper surface. The lifetime distribution for the entire set of trajectories could then be converted, in the usual way,[21] into an overall rate constant for hole or ET. Such a simulation would also handle systems for which decay of the initial state was nonexponential, and for which there consequently would exist no well-defined overall rate constant.

A calculation that adopts this strategy will be reported shortly. However, the special properties of the radical ions **1**−**3** suggest a simpler, albeit more approximate, method of estimating the desired rate constants. Since a single frequency appears to dominate the encounter with the avoided crossing for radical ion **1**, and since the HT is judged to be effectively adiabatic and activationless, it appears that a reasonable estimate of the hole-transfer rate constant would be simply the frequency of encounter with the avoided crossing, i.e. 1458 cm^{-1} or about 4 $\times$ 10^{13} s^{-1}.

Application of the Model to Radical Ions 2 and 3

The graph of $\Delta E(t)$ for a trajectory run on radical ion **2** with ZPE in all normal modes is shown in Figure 6. This plot is similar to that in Figure 4, except that it appears to maintain periodicity for a longer time. The reason is that the radical ion does not encounter the region of the avoided crossing during the trajectory and, hence, cannot undergo the HT. That the failure to encounter the avoided crossing is due neither to the particular phases of the zero-point vibrations selected for this trajectory nor to the relatively brief duration of the trajectory (which was actually followed for 500 fs) can be seen when one compares energies of the C_s and C_{2v} structures for **2**. The C_{2v} geometry, again a local minimum,[22] is found to be 2.56 kcal/mol above the C_s minimum at the AM1 level. This is greater than the ZPE of the antisymmetric combination of π-bond stretching vibrations, which, as before, is the principal contributor to the reaction coordinate for HT. Thus the only way that a trajectory started with ZPE in all modes could result in HT would be by the quantum-mechanically forbidden leakage of ZPE from other modes into the reaction coordinate.

The hole-transfer rate constant can be estimated, in a manner similar to the calculation on radical ion **1**, from a trajectory run

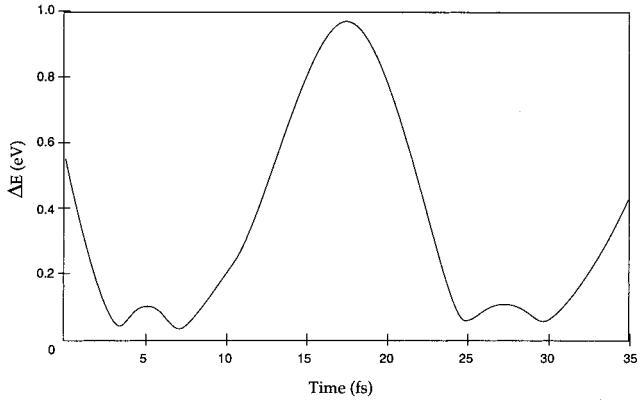

Figure 7. Time dependence of the energy gap between adiabatic states for radical ion **2**, from a trajectory started with ZPE in all modes except the antisymmetric combination of π-bond stretches, which was in $v = 1$. Hole transfer was not permitted at any of the avoided-crossing encounters.

with the critical vibration initially in its $v = 1$ state. The result is shown in Figure 7. Now, as expected, the avoided crossing is encountered, this time with a frequency of about 1500 cm^{-1}. The corresponding harmonic frequency from the normal-mode analysis is found to be 1499 cm^{-1}. With the antisymmetric combination of π-bond stretches in $v = 1$, the system does have a sufficiently large component of its kinetic energy in the direction of the reaction coordinate to access the higher adiabatic surface. The curve in Figure 7 shows the results for a trajectory that does so (i.e., is deliberately prevented from undergoing HT). The "notches" that occur in the minima of the $\Delta E(t)$ curve are a result of the reencounters with the avoided crossing region that inevitably accompany the surface hops (e.g., trajectory C in Figure 2; vide supra).

The fraction, f, of molecules having at least enough energy to populate the $v = 1$ state of the antisymmetric combination of π-bond stretches can be calculated from the expression in eq 7, where $\Omega_{\tilde{\nu}}$ is the number of vibrational states at frequency

$$f = \frac{\sum_{\tilde{\nu}=\tilde{\nu}_{crit}} \Omega_{\tilde{\nu}} e^{-hc\tilde{\nu}/k_B T}}{\sum_{\tilde{\nu}=0} \Omega_{\tilde{\nu}} e^{-hc\tilde{\nu}/k_B T}} \qquad (7)$$

(in cm^{-1}) $\tilde{\nu}$ above the zero point. The denominator of the expression for f is, of course, the vibrational partition function. The numerator is similar, except the summation begins at the frequency $\tilde{\nu}_{crit}$, which is the frequency of the mode responsible for driving the HT, in this case 1500 cm^{-1}. Using the Beyer−Swinehart direct-count algorithm[23] with a step size of 1 cm^{-1} to evaluate $\Omega_{\tilde{\nu}}$, one finds a value of 0.79 for f at 25 °C. In principle this is a simple multiplication factor that reduces the overall rate constant for HT. However, such a calculation ignores the question of where the excess energy is located, and so its use implies the assumption that intramolecular vibrational-energy redistribution (IVR) is fast with respect to HT.

For the trajectory depicted in Figure 7, the overall Landau−Zener total probability, P, for each multiple encounter with the avoided crossing is found to average 0.035, giving an estimated microcanonical rate constant for HT from this state ($Pc\tilde{\nu}_{crit}$) of 1.6 $\times$ 10^{12} s^{-1}. This may well be of similar magnitude to the IVR rate, and so the assumption of fast IVR followed by rate-

(21) Bunker, D. L. *Methods Comput. Phys.* **1971**, *10*, 287.

(22) The existence of the C_{2v} local minimum is again supported by UHF/6-31G(d) ab initio calculations.

(23) *Theory of Unimolecular and Recombination Reactions*; Gilbert, R. G., Smith, S. C., Eds.; Blackwell Scientific Publications: Boston, MA, 1990.

limiting HT is not strictly justified. Nevertheless, we make this approximation because the full trajectory calculation on states with different distributions of internal energy is not currently computationally feasible for a molecule as big as **2**. The overall hole-transfer rate constant ($fPc\tilde{\nu}_{crit}$), which can be seen to be an upper limit because of the assumption about fast IVR, is 1×10^{12} s^{-1}.

Before leaving the discussion on HT in **2**, it is perhaps worth pointing out that the trajectory calculations show clear vibrational-mode selectivity in the hole-transfer event. Thus, a trajectory started with the symmetric combination of π-bond stretches in its $v = 1$ state, and all others in $v = 0$, does not encounter the avoided crossing within the first 500 fs, despite the fact that the total energy is higher than that for the trajectory leading to Figure 7, for which an avoided-crossing encounter occurs within 3.5 fs. This observation further leads one to doubt the validity of the fast-IVR approximation for HT in **2**.

Calculations on radical ion **3** gave results qualitatively similar to those for **2**. A trajectory started with all modes in $v = 0$ did not encounter the avoided crossing, as expected since the C_{2v} structure (this time a transition structure) is 3.14 kcal/mol above the C_s minimum, according to the AM1 model. A trajectory started with the antisymmetric combination of π-bond stretches in $v = 1$ encountered the avoided crossing with the same frequency as that found for **2**, i.e. 1500 cm^{-1} or 4.5×10^{13} s^{-1}. This time, the overall Landau−Zener probability at each double encounter was 0.0029. The fraction of molecules having vibrational energy of 1500 cm^{-1} at 25 °C was found to be 0.91, giving an overall estimate for the hole-transfer rate constant of 1×10^{11} s^{-1}.

While no exact experimental values for the HT rate constants in **1** to **3** are available, it is known that HT through rigid 10-σ-bond frameworks such as that in **3** can occur on sub-nanosecond time scales.[24]

Relationship between Barrier Heights and Electronic Coupling Matrix Elements

For a series of related compounds (specifically, compounds with similar values for the Marcus reorganization energy, λ), one could expect that the barrier height and the matrix element H_{12} should have an approximately constant sum, as illustrated in Figure 8. Thus, as H_{12} decreases, the barrier height on the lower adiabatic surface should increase by a similar amount. This relationship is found to hold to within about 10% for the AM1 calculations on compounds **1**−**3**: for compound **1**, the barrier height is 1.38 kcal/mol and H_{12} is 2.06 kcal/mol (half the energy gap between the adiabatic states at the C_{2v} geometry), summing to 3.44 kcal/mol. For radical ion **2**, the corresponding numbers are 2.56 and 0.66 kcal/mol (sum 3.22 kcal/mol), while for compound **3**, they are 3.14 and 0.16 kcal/mol (sum 3.30 kcal/mol). Thus, the increasing barrier to HT in the series **1** to **3** can be ascribed mostly to the decrease in H_{12}, which is, in turn, due to the increasing number of σ bonds separating donor and acceptor π bonds.

Hole Transfer in Radical Cation 4

The special insight that an MD approach to intramolecular electron (or hole) transfer can afford begins to be revealed when one studies the HT in radical ion **4**.

Even though it belongs to a somewhat different structural series from that for which **1**−**3** are members, the approximately constant sum of barrier to HT and electronic coupling matrix element holds for **4** too. The energy difference between C_{2v} and C_s structures is found to be 2.03 kcal/mol, while H_{12} has a value of 1.22 kcal/mol, giving a sum of 3.25 kcal/mol. The smaller H_{12} for **4** than for **1** reproduces what is observed in ΔE_π values obtained from HF/3-21G Koopmans' theorem calculations on the neutral dienes, and has been ascribed to destructive interference between the parallel σ-bond paths for HT.[9e,f]

The relatively large barrier on the lower adiabatic surface for **4** leads one to expect that a trajectory started with all modes in $v = 0$ will not experience HT. This expectation is verified by running such an MD calculation, but the usual plot of ΔE vs time that results (Figure 9) shows much more complexity than those for radical ions **1**−**3**. The Fourier transform[25] of this waveform (Figure 10) reveals significant contributions from

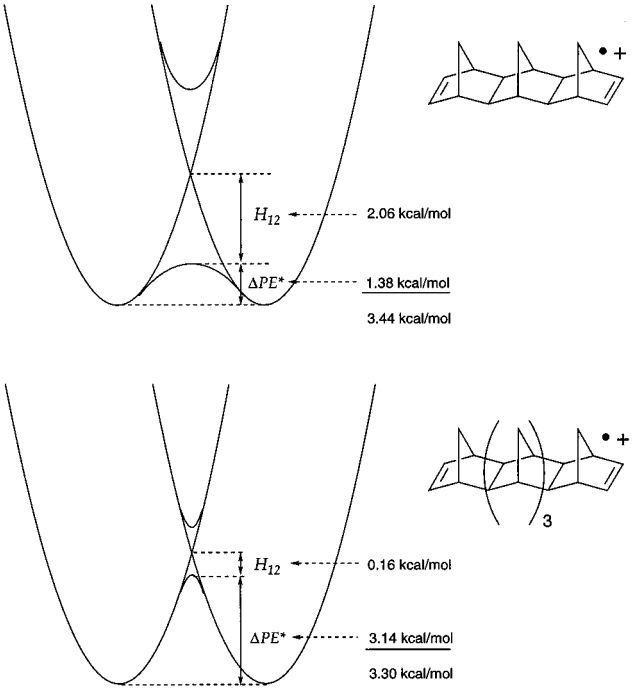

Figure 8. Schematic depiction of the approximation that the barrier to hole transfer on the lower adiabatic surface and the electronic coupling matrix element should sum to a constant value for a series of related compounds. Thus, as the coupling becomes attenuated by distance between donor and acceptor, the barrier should increase.

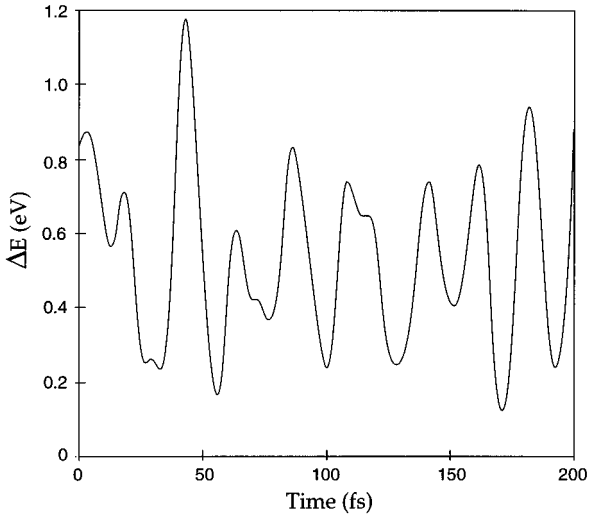

Figure 9. Time dependence of the energy gap between adiabatic states for radical ion **4**, from a trajectory started with ZPE in all modes.

(24) Warman, J. M.; Hom, M.; Paddon-Row: M. N.; Oliver, A. M.; Kroon, J. *Chem. Phys. Lett.* **1990**, *172*, 114.

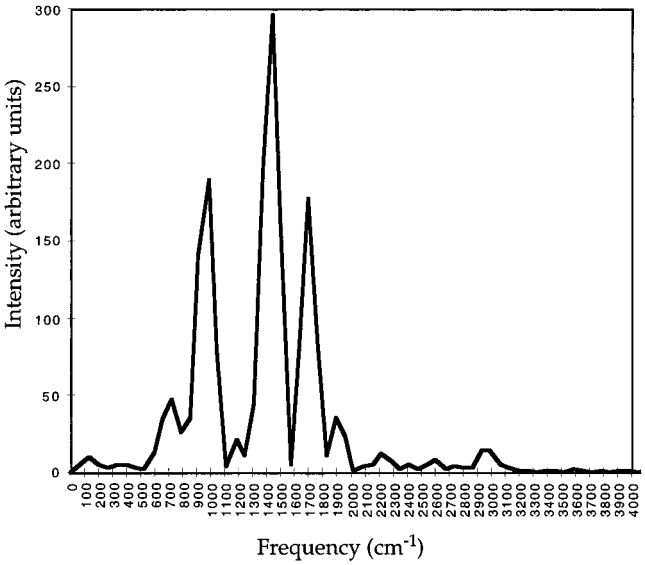

Figure 10. Fourier transform of the waveform shown in Figure 9.

frequencies close to those of the π-bond stretches. In addition, it shows a strong dependence on a mode of frequency around 950 cm^{-1}. There are several skeletal normal modes whose harmonic frequencies are near this value, but the identities of the ones having the largest influence on the energy gap between adiabatic states are easily determined by running trajectories that have ZPE in only one mode at a time. Such a survey reveals that three modes of harmonic frequency 888, 947, and 1150 cm^{-1} have significant modulating effects on the energy gap. Examination of these modes reveals that they all have substantial contributions from C3−C10 stretching.

With hindsight, it is not surprising that C3−C10 stretching should have an influence on the energy gap. It has been shown that the electronic coupling between the π orbitals in dienes such as **1**−**4** is affected by the presence of interference interactions occurring between the dual σ-bond paths linking the π orbitals. This interference, shown schematically by **5** and **6**, increases with decreasing interpath separation.[9e,f] For topolo-

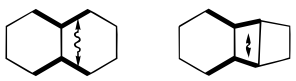

5 **6**

gies such as that in **4**, the interpath interactions are net destructive (although for others, constructive interference is expected[9e,f]). The destructive interference between the hole-transfer pathways is substantially stronger in radical cation **4** than in **1** because the C3−C10 bond in the former holds the dual σ-bond paths between donor and acceptor close and thereby permits efficient interpath destructive interactions. As the C3−C10 bond stretches and contracts during molecular vibration, the interpath interactions are modulated, and this in turn influences the energy gap between the adiabatic electronic states. This phenomenon is revealed in Figure 11, which depicts both the energy gap and the C3−C10 bond length as a function of time from a trajectory that was started with ZPE only in the 947 cm^{-1} normal mode. While the energy gap shows somewhat more complex time dependence than the bond length does, it is clear that the two are in phase and that, as expected from the analysis above, a longer C3−C10 bond leads to a larger energy gap.

(25) Osguthorpe, D. J.; Dauber-Osguthorpe, P. *J. Mol. Graphics* **1992**, *10*, 178.

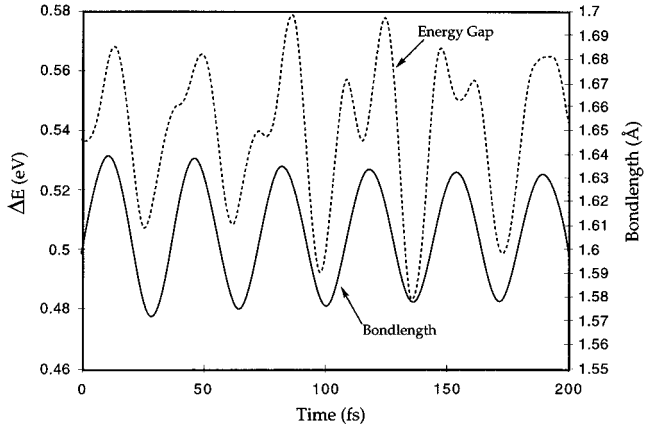

Figure 11. Correlation of C3−C10 bond length changes with energy-gap fluctuations in radical ion **4** for a trajectory started with ZPE only in the normal mode of harmonic frequency 947 cm^{-1}.

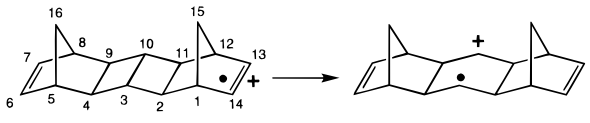

4 **7**

The strong coupling of C3−C10 stretching to the reaction coordinate for HT has another consequence. After 200 fs, for this trajectory, the C3−C10 bond actually breaks, generating the distonic radical ion **7**. It is not clear whether this event mirrors reality, but it is known that ionization of bicyclo[2.2.0]-hexane does result in scission of the corresponding bond.[26] At the UB3LYP/3-21G level, the C_{2v} $^2B_2$ state of **4** is a minimum; however, only 3.2 kcal/mol higher is a $^2A_1$ state that is unstable with respect to cleavage of the C3−C10 bond.

The interactions among the principal modes responsible for the energy-gap modulation in **4** lead to an overall time dependence of ΔE that is not well described by a simple sinusoidal function. This means that the approximate method used to estimate the HT rate constants in **1**−**3** is not really applicable to **4**. It also implies that HT in **4** may not be well described by theories which assume that the relevant high-frequency vibrations in the reactant state may be replaced by a single averaged vibrational mode.[27]

The more rigorous MD method, in which HT is tracked explicitly in trajectories run from a canonical ensemble of starting states, would be applicable to the computation of the overall rate constant were it not for the ring opening reaction, which would probably terminate some trajectories before HT was complete. The participation of the C3−C10 bond in the HT also suggests that a better quantum-mechanical description would result if one used a larger CI space.

Summary

We have descibed in this paper a molecular-dynamics method, employing AM1 semiempirical molecular orbital theory with 2 × 2 CI, that can be applied to intramolecular electron and hole transfer in relatively large molecules. The AM1-CI model appears to do better than the ab initio UHF calculations (see Supporting Information) in describing barrier heights to HT because the use of the "half-electron" model in the AM1 calculations avoids the problem of doublet instability that

(26) Williams, F.; Guo, Q.-X.; Bebout, D. C.; Carpenter, B. K. *J. Am. Chem. Soc.* **1989**, *111*, 4133.

(27) Jortner, J. *J. Chem. Phys.* **1976**, *64*, 4860.

appears to make the C_{2v} structures spuriously high in energy when described by a standard UHF wave function.

For molecules such as **1**−**3** the calculations reveal that the common assumption of a single, well-defined encounter frequency with the avoided crossing is probably justified. However for molecules such as **4** this approximation is seen to be unwarranted and complex time dependence of the energy gap ΔE, is observed. Nevertheless, such complex behavior should provide deeper and rewarding insights into the factors that govern electron-transfer dynamics, such as the electronic coupling between different paths for electron transfer. This is certainly the case for the cation radical **4**, where our dynamics study nicely corroborates the existence of destructive interference effects in this system which were predicted using only a simple model based on Koopmans' theorem.[9e,f]

In general, flexible molecules, or molecules for which ET would be symmetry forbidden in the stationary-state geometry (such as radical ion **8**), are also likely to show complex time dependences of the energy gap ΔE and hence are unlikely to be well described by models that ignore explicit molecular dynamics. Indeed, photoinduced energy and ET processes in dinuclear ruthenium(II) and/or osmium(II) complexes connected to the bridge depicted by **8** have been found to occur readily on a nanosecond time scale.[28] These results certainly indicate that the formally symmetry forbidden transitions are in fact occurring quite well, presumably by vibrational modes that remove the offending symmetry. The technique described here, when implemented in its more rigorous form, promises to provide ways of probing such problems.

The ability to dissect the energy gap fluctuations, and hence the overall rate constant for hole or ET, into components dependent on particular vibrational normal modes is of special interest. One could anticipate, among other possibilites, that such analyses would allow one to make predictions about isotope effects on the overall rate constant. It is even conceivable that one could find molecular systems in which ET would be formally symmetry forbidden, but for which certain vibrational modes would lead to distorted structures from which very rapid transfer would occur. For such molecules one might be able to influence the electron-transfer rate constant by pumping specific modes with an IR laser. Whether **8** or some of its derivatives belong to such a class of molecular systems is a question under current investigation.

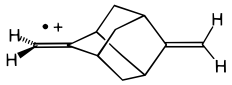

8

Although the present paper is concerned with degenerate HT reactions, there is no obvious reason why the technique described here should be limited to such processes. Nondegenerate reactions as well as ETs in radical anions should be relatively straightforward to study by similar methods. The more interesting reactions in which electronic excited states decay to charge-separated states could also be studied, provided one used a semiempirical MO procedure that was parametrized to describe the excited states reasonably.

We are actively applying our AM1-based molecular-dynamics method to these and other contemporary issues in ET research,[29] and because conclusions based on single trajectory calculations should be treated with caution, we are extending our calculations of hole-transfer and electron-transfer rate constants to cover ensembles of trajectories. In addition, we are exploring implementation of some of the more sophisticated models of nonadiabatic dynamics,[3] using the AM1 CI density matrices.

Acknowledgment. We thank the Australian Research Council (ARC) and the National Science Foundation (Grant No. CHE-9528843) for support of this work. G.A.J. also acknowledges receipt of an ARC postgraduate award. We acknowledge the New South Wales Centre for Parallel Computing for use of the Silicon Graphics Power Challenge.

Supporting Information Available: Table of angles between the momentum-correction vector, **n**, and the normal modes for the C_{2v} geometry of radical ion **1** and comparison of HF and B3LYP calculations with AM1-CI calculations for radical ions **1**−**4** (5 pages, print/PDF). See any current masthead page for ordering information and Web access instructions.

JA9737533

(28) (a) De Cola, L.; Balzani, V.; Barigelletti, F.; Flamigni, L.; Belser, P.; Bernhard, S. *Recl. Trav. Chim. Pays-Bas* **1995**, *114*, 534. (b) Balzani, V.; Barigelletti, F.; Belser, P.; Bernhard, S.; De Cola, L.; Flamigni, L *J. Phys. Chem.* **1996**, *100*, 16786.

(29) Barbara, P. F.; Meyer, T. J.; Ratner, M. A. *J. Phys. Chem.* **1996**, *100*, 13148.